REPORT DOCUMENTATION PAGE

Form Approved OMB No. 0704-0188

1. REPORT DATE *(DD-MM-YYYY)*	2. REPORT TYPE	3. DATES COVERED *(From – To)*
27-07-2010	Final Report	23 July 2009 - 23-Jul-10

4. TITLE AND SUBTITLE

Low Noise Optically Preamplified Lightwave Receivers and other Applications of fiber optic parametric amplifiers

5a. CONTRACT NUMBER
FA8655-09-1-3076

5b. GRANT NUMBER

5c. PROGRAM ELEMENT NUMBER

6. AUTHOR(S)

Professor Peter Andrekson

5d. PROJECT NUMBER

5d. TASK NUMBER

5e. WORK UNIT NUMBER

7. PERFORMING ORGANIZATION NAME(S) AND ADDRESS(ES)

Chalmers University of Technology
Kemivagen
Gotghenbur 41296
Sweden

8. PERFORMING ORGANIZATION REPORT NUMBER

N/A

9. SPONSORING/MONITORING AGENCY NAME(S) AND ADDRESS(ES)

EOARD
Unit 4515 BOX 14
APO AE 09421

10. SPONSOR/MONITOR'S ACRONYM(S)

11. SPONSOR/MONITOR'S REPORT NUMBER(S)
Grant 09-3076

12. DISTRIBUTION/AVAILABILITY STATEMENT

Approved for public release; distribution is unlimited.

13. SUPPLEMENTARY NOTES

14. ABSTRACT

Optical amplifiers are key elements in many types of optical systems including optical fiber communication links and laser-based radars. Some of the most important aspects of such amplifiers are their noise performance, optical bandwidth, and power efficiency. During this year, we propose to both extend previous work and initiate new activities. Our work on broadband FOPAs recently resulted in a world record optical bandwidth of over 80 nm (the pump wavelength separation was 103 nm) with 40 dB of gain. We will try to extend this further by extending the wavelength separation of the two pump lasers of the FOPA. To date, our results were limited essentially only by our practical laboratory limitations and not by the inherent properties of the highly nonlinear fiber that provides the gain medium. We now expect to be able to increase the pump separation to 150 nm and beyond and then the internal fiber parameters, such as fourth-order dispersion, zero-dispersion wavelength variation along the fiber, PMD, and certainly stimulated Raman scattering will emerge as limiting factors for the possible gain bandwidth. We may possibly evaluate such a very broadband amplifier as a gain medium in a very widely tunable laser by incorporating it in a cavity with external mirrors. A natural extension of our work on saturation of FOPAs is to investigate its intensity regeneration features, perhaps in particular in the context of phase modulated signals. We will further expand our work to implement phase-sensitive FOPAs. While such amplifiers have intriguing properties, in particular a quantum-limited noise figure of 0 dB, their implementation is very challenging. We will approach this with a so-called non-interferometric approach by using three different optically phase controlled waves of very high coherence at the input stage.

15. SUBJECT TERMS

EOARD, Fibre Optics, Laser Communications, Nonlinear Optics

16. SECURITY CLASSIFICATION OF:			17. LIMITATION OF ABSTRACT	18, NUMBER OF PAGES	19a. NAME OF RESPONSIBLE PERSON
a. REPORT	b. ABSTRACT	c. THIS PAGE			A. GAVRIELIDES
UNCLAS	UNCLAS	UNCLAS	UL	16	19b. TELEPHONE NUMBER *(Include area code)* +44 (0)1895 616205

Low Noise Optically Pre-amplified Lightwave Receivers and Other Applications of Fiber Optic Parametric Amplifiers

Award No.: FA8655-1-3076
Carl Lundström, Zhi Tong, Ben Puttnam, and Peter A. Andrekson

Photonics Laboratory, Department of Microtechnology and Nanoscience
Chalmers University of Technology
SE-412 96 Göteborg, Sweden

Period covered: July 23, 2009 – July 22, 2010

***Abstract* — We report on our progress in fiber optical parametric amplifiers (FOPAs) in both phase-insensitive (PI) and phase-sensitive (PS) configurations. Direct phase-squeezing performance was characterized experimentally in PS-FOPAs. We have further developed a technique to accurately measure the noise figure (NF) of these amplifiers. With this we have extensively characterized the spectral features of the NF in FOPAs. A record low NF = 1.1 dB was measured in a high-gain (26 dB) PS-FOPA. We also propose the application of PS-FOPAs in transmission systems which would lead to up to 6 dB link SNR improvement.**

I. Introduction

Optical amplifiers are key elements in many types of optical systems including optical fiber communication links and laser-based radars. Some of the most important aspects of such amplifiers are their noise performance, optical gain bandwidth, and power efficiency. An interesting alternative to the mature Erbium-doped fiber amplifier (EDFA) is the fiber optic parametric amplifier (FOPA), which has significantly different characteristics since it relies on nonlinear interaction in a fiber. As a consequence, it can be tailored to operate, in principle, at any wavelength and thereby opens up new wavelength bands for amplification with applications within and outside telecom. The first CW pumped FOPA was presented in [1], and was facilitated by the new dispersion controlled highly nonlinear fibers (HNLF) and high power booster EDFAs. The FOPA can provide a very wide gain bandwidth [2], very high gain (70 dB was demonstrated in [3]), and ultimately a 0 dB noise figure when operating in phase sensitive mode, even though this is difficult in practice since it requires tracking of the optical signal phase [4]. A phase-sensitive FOPA will also squeeze the signal phase, thus providing phase regeneration. The nonlinear response time of the FOPA is very fast (femtosecond-range), which may prevent it from being operated in saturated mode in wavelength division multiplexed (WDM) systems [5], but, on the other hand, opens up many possibilities for multi-functional all-optical signal processing, besides pure amplification, for example pulse generation, de-multiplexing, wavelength conversion and optical sampling [6].

The single pumped (or degenerate) FOPA relies on a strong pump signal at the wavelength λ_p, which should be placed near the zero-dispersion wavelength, λ_0, of the gain fiber for broadband amplification around the pump wavelength. It is combined with a weaker signal at λ_s, which experiences gain while an idler wave is generated at $\lambda_i \approx 2\lambda_p - \lambda_s$ when the pump power is transferred to the signal and idler wavelengths, according to Fig. 1.

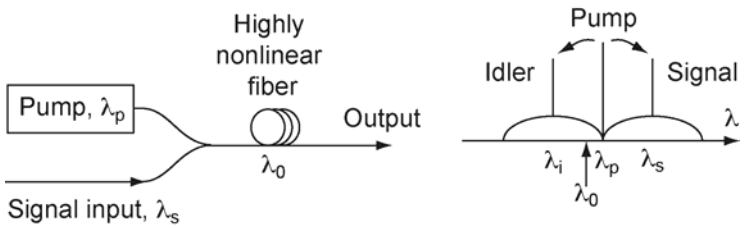

Fig.1. (left) Schematic setup of the single pumped FOPA with the combination of the pump and signal. (right) The principle output spectrum with the generated idler, and noise.

A noise floor similar to the amplified spontaneous emission (ASE) noise in EDFAs is also generated. It is sometimes referred to as amplified quantum noise. Maximum gain (at the gain peak) is obtained when perfect phase matching is achieved in the single pumped configuration, and it is approximately given by

$$G_0 \approx \frac{1}{4}\exp(2\gamma P_p L). \quad (1)$$

The gain is lower close to the pump wavelength and is approximately given by

$$G \approx (\gamma P_p L)^2. \quad (2)$$

At the peak, the gain grows exponentially with the product $\gamma P_p L$, where γ is the nonlinearity parameter ($W^{-1}km^{-1}$) of the HNLF, P_p is the pump power (W) used to excite the FOPA, and L is the length of the HNLF (in km). For a 500 m long fiber with a γ of 10 $W^{-1}km^{-1}$ and a pump power of 1 W, one could in theory reach a gain of 37 dB. Close to the pump, where the gain grows quadratically with pump power, the expected gain for the same parameters is only 14 dB. Hence, only over a limited region around the peak gain it can be regarded as flat. Note that the peak gain wavelength, the bandwidth, and the gain flatness depend on many parameters; for example the wavelength separation between the pump wavelength and the zero dispersion wavelength, the dispersion slope, the pump power, and the fiber length. It may still be difficult to achieve high, broad, and flat gain in practice due to fourth-order dispersion and zero-dispersion wavelength variation in the fiber. The double pumped configuration is more attractive if broad and flat gain is desired.

The double pumped FOPA relies on two strong pump signals at the wavelengths λ_{p1} and λ_{p2}, where the spectral center-of-gravity should be placed near the zero-dispersion wavelength of the gain fiber for broad and flat gain. They are combined with a weaker signal at λ_s, which experiences gain while an idler wave is generated at $\lambda_i \approx \lambda_{p1}+\lambda_{p2}-\lambda_s$ when the power is transferred from the pumps to the signal and idler, according to Fig. 2. In contrast to the single pumped FOPA, the gain of the double pumped configuration can be almost flat between the pumps. The flatness is determined mainly by the fourth-order dispersion, and the zero-dispersion wavelength variation in the HNLF.

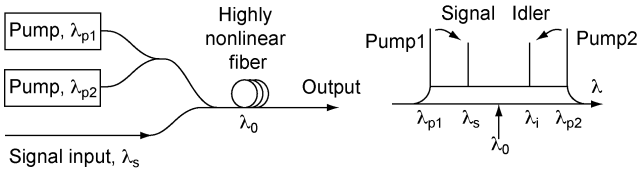

Fig. 1. (left) Schematic setup of the double pumped FOPA with the combination of the pumps and signal. (right) The principle output spectrum with the generated idler, and noise.

In the special case of equal pump power, $P_{p1}=P_{p2}=P_p$, the flat gain between the pumps is given by

$$G_0 \approx \frac{1}{4}\exp(4\gamma P_p L). \quad (3)$$

Hence, for a total pump power of $P_{p1}+P_{p2}$ = 1 W (0.5W + 0.5W), a γ of 10 $W^{-1}km^{-1}$, and L = 500 m, we expect a signal gain of 37 dB.

A FOPA operating in phase-sensitive mode, offering among other things the aforementioned 0 dB quantum limited noise figure, is in principle constructed in the same way as the conventional FOPAs described above, with the important difference of having the idler present at the input. However, since the interaction is dependent on the relative phase of the waves, all three or four ingoing waves must be phase-locked, which is the biggest challenge in implementing PS-FOPAs. Typically, we consider two different configurations of PS-FOPAs; the degenerate-idler and the nondegenerate-idler configurations. In the former, the signal and idler are degenerate and symmetrically surrounded by two pumps. This case is convenient, since there is no need for two waves carrying the same data, but it is inherently a single channel device. The nondegenerate-idler configuration can provide phase-sensitive amplification to many signal-idler pairs simultaneously, but generating a data-carrying idler is challenging.

In Sec. II we detail our recent advances using parametric wavelength conversion to generate widely separated pumps to achieve ultra-wideband amplification. It was found that fundamental fiber properties limited the amplification bandwidth. In Sec. III, a detailed investigation of the noise performance of single-pumped FOPAs is presented. For the first time, an asymmetric NF spectrum induced by both Raman induced excess noise and Raman modified pump transferred noise of a fiber parametric amplifier was measured, in good agreement with theory. In Sec. IV, advances in implementing phase-sensitive (PS) FOPAs are discussed, and the phase-squeezing behavior of PS-FOPAs is characterized in Sec V. In Sec. VI, we present measurements of the noise figure of a PS-FOPA in a cascaded configuration. When measuring the NF of the signal or idler separately, a negative noise figure was measured. However, when considering the combined signal-idler mode (since both need to be present at the PSA input), an NF of 1.1 dB was measured, still well below the conventional 3 dB-quantum limit of any conventional phase-insensitive amplifier. Finally, in Sec. VII, our ongoing work in implementing PS-FOPAs as transmission amplifiers is presented.

II. ULTRA-WIDEBAND AMPLIFICATION

The parametric amplifier can in the dual-pump configuration in principle exhibit gain over arbitrarily wide optical bandwidths, with spectrally flat gain in the optical bandwidth between the two pumps. Furthermore, the gain will be exponential with respect to the nonlinear phase shift in the fiber. However, in practice there will be other effects that limit both the bandwidth and the flatness of the gain. We have invested a large amount of work and hardware to develop the dual-pumped FOPA set-up shown in Fig. 3. This allows us to operate the dual-pumped FOPA over a wide range of pump separations ($\Delta\lambda$), with about 1W of optical power from each pump. In the simplest case, the two high power pumps (λ_1 and λ_4) are amplified directly by a C-band and an L-band booster EDFA, respectively. This, however, limits the attainable pump separation to about 70 nm. To increase the pump separation further one or both of the pumps can be wavelength converted using a first stage single-pumped FOPA to λ_3 and λ_6, respectively, outside of the gain bandwidths of conventional EDFAs. By combining a multi-watt pump with a signal of at least 1W into an HNLF of 50-100 m length, an idler wave of approximately 1W can be generated, and subsequently filtered out for use as a pump in the dual-pumped FOPA (the second stage). All high-power waves were externally phase modulated prior to amplification to avoid Stimulated Brillouin Scattering (SBS). The HNLF used for the double-pumped FOPA is a state-of-the-art fiber and has the following parameters: L = 350 m, A_{eff} = 9.4 μm^2, S_0 = 0.025 ps/nm^{2}km, λ_0 = 1561.9 nm, $\beta_4 = 2.5*10^{-5}$ ps^4/km, estimated variation of λ_0 of below 1 nm and a measured differential group delay (DGD) of 0.031 ps.

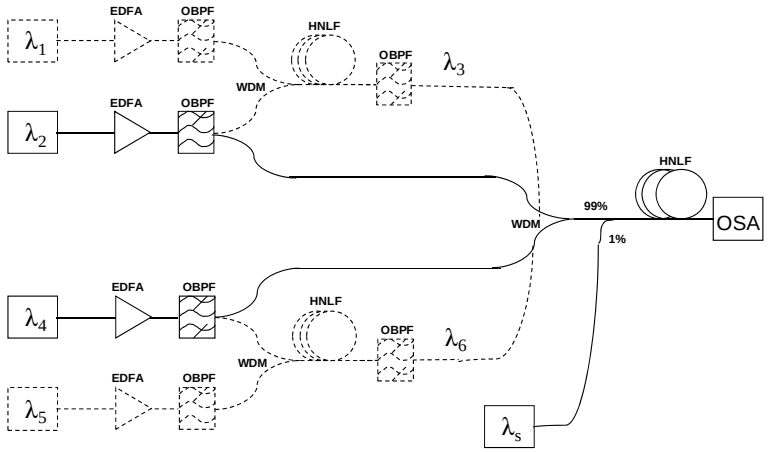

Fig. 3. Simplified schematic setup of the double pumped FOPA. EDFA: Erbium doped fiber amplifier, OBPF: optical band pass filter, WDM: wavelength division multiplexer, HNLF: highly nonlinear fiber. The pumps are either directly injected into the HNLF after EDFA amplification (solid lines) or wavelength converted in a first stage HNLF (dashed lines).

We have previously published results when wavelength converting one pump down to the S-band (approximately 1511 nm), with the other pump being directly amplified with an L-band EDFA [7]. In this configuration, the pump separation was limited to 103 nm. A flat (ripple below 1dB) gain spectrum between the pumps with a 3dB-bandwidth of 81 nm was then measured. However, the flatness of the gain spectrum was very sensitive to the pump wavelength detuning, with a shift of only less than one nanometer visibly distorted the gain spectrum.

We have also implemented a FOPA with up to 150 nm pump separation utilizing FWM-based wavelength conversion for both pumps. The pump wavelengths were λ_3 = 1489.3 nm and λ_6 = 1639.8 nm, while the pump powers were approximately 700 mW each. The pump wavelengths were optimized to produce the flattest parametric gain possible between the pumps. In Fig. 4 the total on-off gain (squares), parametric gain (circles) and the Raman gain from pump 1 (diamonds) are shown. The parametric gain is larger close to the pumps and decreases to less than 10 dB over the major part of the center lobe, indicating that good phase matching is not possible over the entire center lobe, due to the combined influence of fourth-order dispersion and variations of λ_0. As the peak Raman gain is also 10 dB and located at 1594 nm, the total gain spectrum is significantly distorted by the Raman gain. Reducing the power of pump 1 (P_1) but maintaining the product $(P_1P_2)^{1/2}$ can improve the flatness of the total gain, as the Raman gain produced by pump 1 is reduced, but the parametric gain maintained.

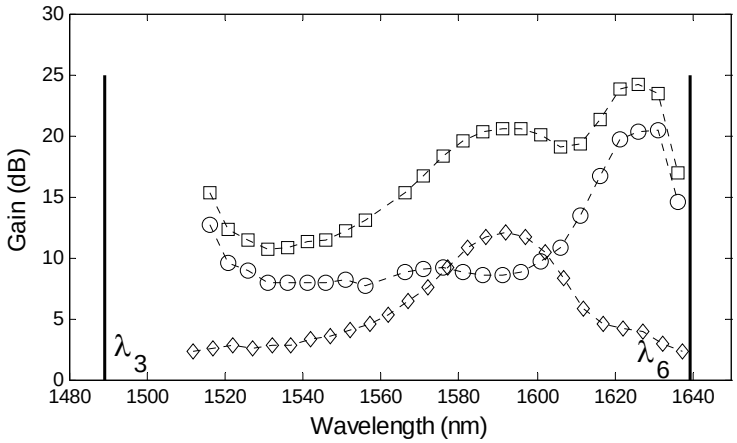

Fig. 4. Measured parametric (circles), Raman (diamonds) and total (squares) gain spectra of using a pump separation of 150 nm. Lines indicate pump wavelength allocations.

We conclude, that since the parametric gain with the Raman contribution removed exhibits a large and wide reduction in the central part of the gain spectrum, this pump separation is not possible to achieve with this particular fiber, despite its very good characteristics, notably its low β_4 and small variation of λ_0. The impact of β_4 on the phase-matching can in principle be compensated for by detuning the pump center-of-gravity relative to the λ_0 of the fiber, but the existence of λ_0–variations reduces the ability to do so accurately. Furthermore, the wider the pump separation, the better accuracy of this detuning is needed. There is thus a limit of how much zero-dispersion variations one can accept in order to achieve flat gain, for a given pump separation and β_4L-product. Reducing the length of the fiber is one possible solution, since it reduces the impact of the fourth-order dispersion, and can possibly also reduce the variation of λ_0. The pump powers will then need to be increased to maintain the gain. It is well known that further reductions in variation of λ_0 by improved HNLF manufacturing tolerances is unlikely, since the transverse geometry of the fiber can already be controlled to within molecular dimensions. This thus poses a fundamental limit on the parametric gain bandwidth in HNLFs. The Raman process is another fundamental effect that will affect the gain spectrum. While the relative influence of the Raman effect will reduce if phase matching is good and the parametric gain high, this was may not always be possible. One way of reducing the impact of it may be to position the two pumps approximately 200 nm apart so that the Raman gain from one pump and the Raman attenuation from the other will cancel out to some degree. In conclusion, we have now reached the point where the gain bandwidth of the dual-pumped FOPA is no longer limited by available pumps, but rather by fundamental properties of the HNLF.

III. IMPACT OF ZDW VARIATIONS ON THE NOISE PERFORMANCE OF FOPAS [8]

Noise performance of fiber optical parametric amplifiers (FOPAs) has been extensively studied. Besides the intrinsic amplified quantum noise (AQN), three main excess noise sources have been reported to degrade the noise figure of a FOPA [9], which are Raman phonon induced excess noise, pump transferred noise (PTN) and pump residual amplified spontaneous emission (ASE), respectively. However, most of the previous works ignored ZDW fluctuations in FOPAs, which originate from the longitudinal non-uniformity in the gain fibres, and become an important factor limiting the maximum FOPA gain as well as bandwidth [10]. Velanas *et al.* [11] simulated the NF spectra of FOPAs with random ZDW fluctuations by taking into account both AQN and PTN. They carried out numerous calculations to account for the ZDW statistics and then obtained the average gain and NF, which makes the analysis complicated and time-consuming. When considering the impacts of ZDW distributions on FOPA NF performance, a problem is that different ZDW variations might significantly change the maximum gain as well as the bandwidth, which makes direct NF comparisons unfair (only NF within the gain bandwidth is meaningful). It is better to analyze the NF characteristics with ZDW fluctuations under the same gain spectrum. Marhic *et al.* [12] have proved that the FOPA gain is reciprocal even in presence of arbitrary ZDW variations. This characteristic makes it possible to directly compare the impacts of ZDW distributions on noise performance. Thus, more general conclusions can be expected.

It can be proved that the signal gain as well as AQN remains identical regardless of the pumping directions, even with Raman effect (Raman gain is independent of the phase-mismatching induced by ZDW variations). Both signal and AQN will experience the same gain in either direction. This is also true after adding the PTN contribution, as PTN is related to the derivative of the FOPA gain with respect to pump power, while this derivative remains unchanged when altering the pumping direction. However, the problem will be more complicated when introducing the Raman phonon induced noise.

In Fig. 1 we compare the calculated gain and NF spectra of a typical FOPA with and without ZDW fluctuations. We used 250 m HNLF (with mean ZDW λ_0=1551 nm, nonlinearity coefficient γ=11.7 $W^{-1}km^{-1}$, dispersion slope S_0=0.019 ps/nm^2km, and the peak Raman gain coefficient is 4.5 $W^{-1}km^{-1}$) in calculations as the gain medium. We divided the HNLF into 60 pieces to model the ZDW variations. The pump wavelength was fixed at 1554.5 nm, the input pump power was 1 W and the signal input was -25 dBm to reduce PTN. Here we assumed a 6 nm linearly-changing ZDW along the fiber to simplify the

calculations. This may be a very good approximation of stretched fibers [13]. From Fig. 1, we can see that the gain spectrum is identical in both directions even with ZDW variations and Raman effect when changing the amplification directions, while the NF spectra are different, which clearly shows the noise non-reciprocity of the FOPA. A flatter noise performance can be obtained as the fibre ZDW is in the linearly-decreasing (from 1554 to 1548 nm) distribution. The reason is that ZDW variations will affect the parametric gain at different positions but not the Raman phonon induced noise. A longer ZDW at the input (but still below the pump wavelength, otherwise the FOPA will become inefficient) will give a higher signal gain around the gain edges at the beginning, and thus improve the noise performance there, otherwise the Raman phonon induced noise which is independent of the ZDW distributions will dominate the noise performance in the region relatively far from the pump wavelength.

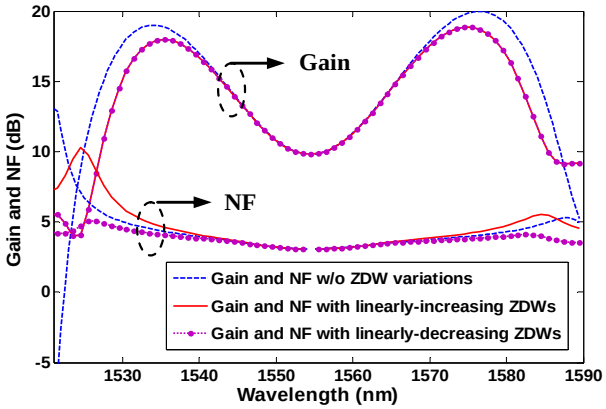

Fig. 5 Calculated gain and NF spectra with or without ZDW variations, which were assumed to be linearly changing from 1548 to 1554 nm.

We also experimentally verified the theoretical simulations. The measurement setup is shown in Fig. 6. A 60 mW output DFB laser (1554.5 nm) was used as the pump laser, which was phase-modulated to suppress the stimulated Brillouin scattering. After an EDFA booster followed by two cascaded filters, the amplified pump was combined with the signal by a 10 dB coupler. To show the impacts of ZDW variations, we combined two HNLF spools with different mean ZDWs (The parameters are: HNLF1, with L=150 m, λ_0=1553.6 nm, γ=10 $W^{-1}km^{-1}$, S_0=0.018 ps/nm^2km, and HNLF2, with L=245 m, with λ_0=1545.5 nm, γ=11.7 $W^{-1}km^{-1}$, S_0=0.02 ps/nm^2km). The output noise spectra of HNLF1, HNLF2 and their combination are shown in insets (a), (b) and (d) of Fig. 3, respectively, for a 1 W input pump power. The splice loss between two fiber spools was less than 0.2 dB. To change the amplification direction, one just needs to exchange the input and output of the combined HNLF spools.

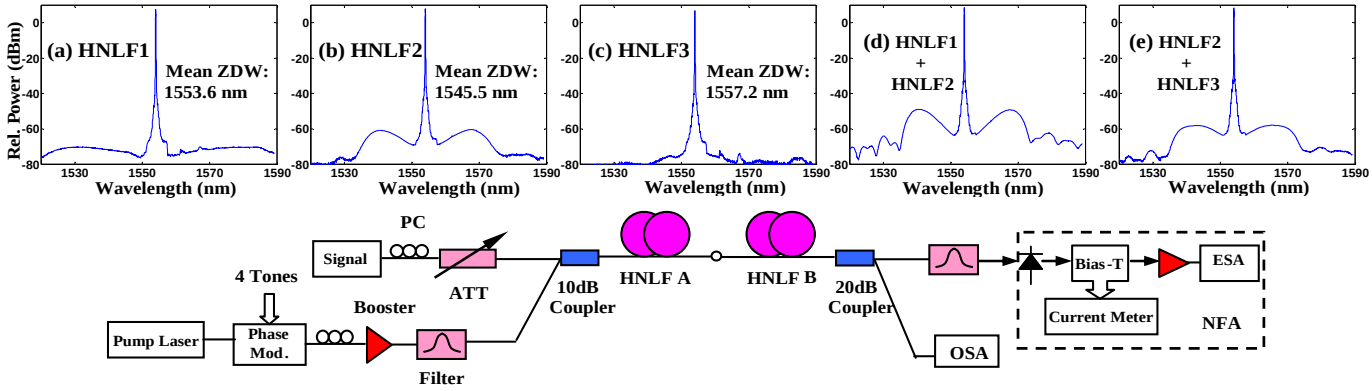

Fig. 6 Measurement setup. NFA: Noise figure analyzer; ESA: Electrical spectrum analyzer; OSA: Optical spectrum analyzer; PC: Polarization controller; ATT: Variable attenuator. Insets (a)-(e) show noise spectra of three individual HNLFs with different ZDWs, and their combinations, respectively.

The calculated and measured gain and NF spectra by changing the pumping direction are shown in Fig. 7. The pump input power was about 0.95 W, while the input signal was -25 dBm. Diverging NF spectra can be clearly seen at different amplification directions, though the gain profiles are almost identical (the gain deviation is due to the distributed HNLF attenuation, which is not included in the theory). It should be noted that this gain difference contributes almost nothing to the NF non-reciprocity. A better NF performance was obtained when using the combination in HNLF1 + HNLF2 order, which agrees well with the theoretical prediction. Experimental results agree with theory very well, and the deviation is probably due to the fiber PMD and the ZDW variations of two HNLFs themselves. Moreover, in Fig. 8 we compared the gain and NF spectra in different FOPA directions by combining HNLF2 with another 200 m HNLF spool (HNLF3, λ_0=1557.2 nm, γ=11.9 $W^{-1}km^{-1}$, S_0=0.016 ps/nm^2⊙km). The pump operated in the normal dispersion regime in HNLF3. The output noise spectra of HNL3 alone and HNLF2 + HNLF3 are shown in inset (c) and (e) of Fig. 6. A strong NF non-reciprocity can be seen from Fig. 8, however, in this case the HNLF3 + HNLF2 combination (which placed the longer ZDW close to input)

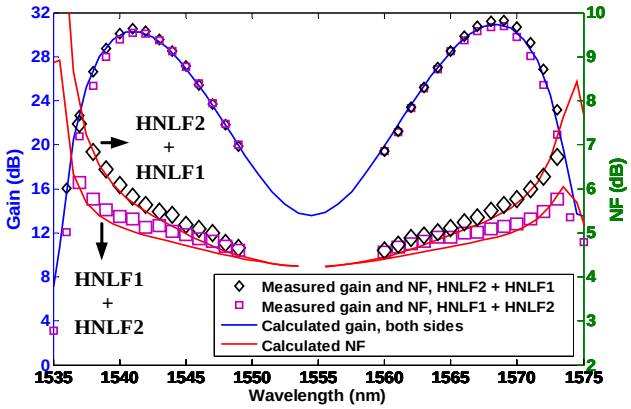

Fig. 7 Measured and calculated gain and NF spectra in different amplification directions with HNLF1 and HNLF2 combined. The NF contribution due to the pump residual ASE was assumed to be 0.6 dB in calculations.

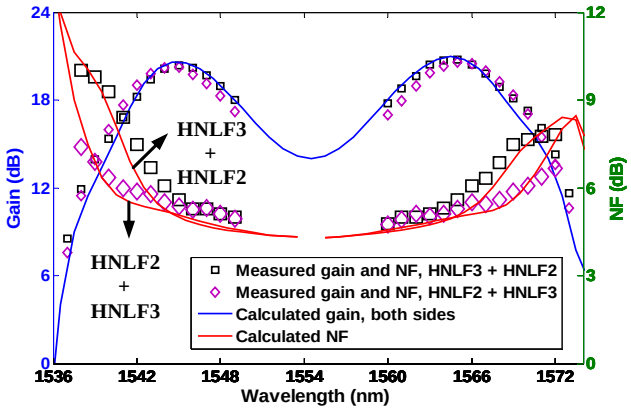

Fig. 8 Measured and calculated gain and NF spectra in different amplification directions with HNLF2 and HNLF3 combination. The NF contribution due to the pump residual ASE was assumed to be 0.6 dB in calculations.

IV. PHASE-SENSITIVE PARAMETRIC AMPLIFICATION

Phase-sensitive amplification have long been known to offer the possibility of amplification with a noise figure (NF) below the 3 dB quantum limit of their PIA counterparts [14]. In addition, considerable interest in them has arisen due to their potential for optical signal processing, including all optical phase regeneration of phase-encoded signals [15-17], dispersion compensation [18] and coherent wavelength exchange [19]. By operating a PSA in saturation, simultaneous phase and amplitude regeneration can be achieved [17, 20-21].

PSA in optical fiber systems can be achieved in a nonlinear optical loop mirror [22]. This interferometric loop configuration has been successfully used to demonstrate both sub-3 dB-NF [4] and phase-regeneration of phase-encoded signals [16-17]. However, an interferometric PSA is inherently single-channel, and thus not compatible with wavelength-division-multiplexed (WDM) systems, and the possibility of achieving sub-3 dB-NF is complicated by their susceptibility to guided acoustic wave Brillouin scattering (GAWBS) [20]. PSA can also be implemented using four-wave mixing in a non-degenerate fiber-optic parametric amplifier (FOPA), avoiding the above two drawbacks of interferometric PSAs. A non-degenerate idler FOPA-based PSA requires the injection of three or four waves; one or two pumps, and a signal-idler pair, which then experience amplification or de-amplification. Several different signal-idler pairs can be phase-sensitively amplified at the same time. A schematic of this configuration is shown in Fig. 10.

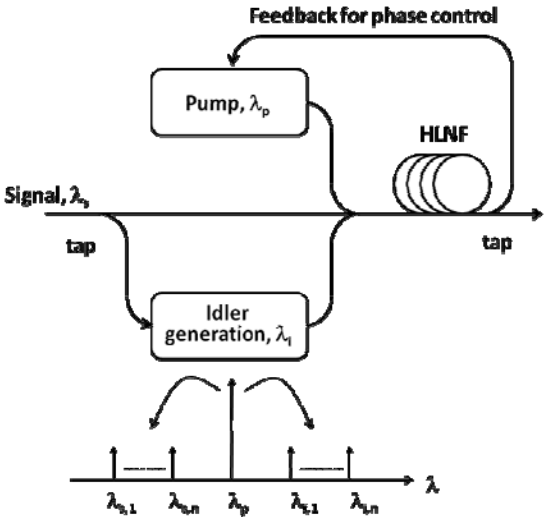

Fig. 10. Schematic of a PS-FOPA in the non-degenerate-idler configuration. All three waves need to maintain a stable phase relationship at the HNLF input.

From simple theory [23] the signal gain can be written as:

$$G_S = 1 + 2\sinh^2(\gamma P L_{eff}) + 2\sinh(\gamma P L_{eff})\cosh(\gamma P L_{eff})\sin(\theta_{rel}) \,, \tag{6}$$

where γ is the nonlinearity coefficient, P is the pump power and L_{eff} is the effective fiber length. The PSA gain or attenuation is governed by the total relative phase, θ_{rel}, among the three interacting waves. It is defined as $\theta_{rel} = 2\varphi_p - \varphi_s - \varphi_i$, with φ_p, φ_s and φ_i being the absolute phases of the pump, signal and idler waves, respectively. θ_{rel} is constant after a PIA, regardless of the changes in phase of the input waves, since all three waves are coupled and the ultrafast response of the FWM process allows it to track very fast variations in phase.

The interacting waves need to be phase-locked for proper PSA operation, which is a significant challenge. This configuration can thus be emulated in a number of ways. Three phase-locked waves can be derived by using electro-optic modulation (EOM) of a narrow linewidth optical source, producing multiple sidebands locked to the carrier. However, current EOM technology limits the bandwidth achievable via this technique to a few 100 GHz at best. A wideband PSA can be created by cascading two FOPAs, generating a phase-locked but conjugated idler in the first FOPA (the so-called copier), and, with a mechanism for changing the relative phase among the waves in between, achieving PSA operation in the second one. Thus, the PSA can be characterized either statically or dynamically, depending on how this intermediate phase change is implemented. However, it should be noted that since the generated idler in the copier is a conjugated copy of the input signal, it is not possible to achieve any phase-sensitive interaction based on the phase of the input signal, since the signal and idler phase will cancel out. The phase-sensitive interaction can only be dependent on the relative phase difference that is introduced among the three waves between the copier and the PSA. It should also be noted that the NF of the combined system will be limited by the 3 dB quantum limit of the PI copier stage.

In [24] we implemented a straight-line cascaded copier+PSA based on two FOPAs. Using an optical processor between the copier and PSA, we could change the relative phase statically between the two stages, thus we could stably measure the phase dependent gain of the second stage, the first time such a measurement was demonstrated. We also measured the gain spectrum of the PSA, and demonstrated a record-high phase-sensitive gain of 33 dB, and also demonstrated a PSA operating in saturation. All these results show that if the problem of stably locking the ingoing waves can be solved, a FOPA-based PSA can exhibit all the performance traits of conventional PI-FOPAS, while at the same time be phase-sensitive.

Any configuration that allows for phase-sensitive amplification in response to a signal rapidly varying in phase, e.g. a multi-gigabit/s phase-encoded data signal requires external phase-locking among the waves. We have implemented such a setup, detailed in Fig. 11. Using a conventional single-pumped FOPA as a first-stage copier, three stably phase-locked waves are generated. By splitting the pump in one arm and the signal and idler in the other using a WDM coupler, fast phase data can be encoded onto the signal and idler simultaneously. By recombining the signal and idler with the pump, and stabilizing the thermally induced slow phase drift between the arms using a piezo-electric transducer (PZT) in a conventional phase-locked loop (PLL) setup stable phase-sensitive interaction can be achieved in the second stage.

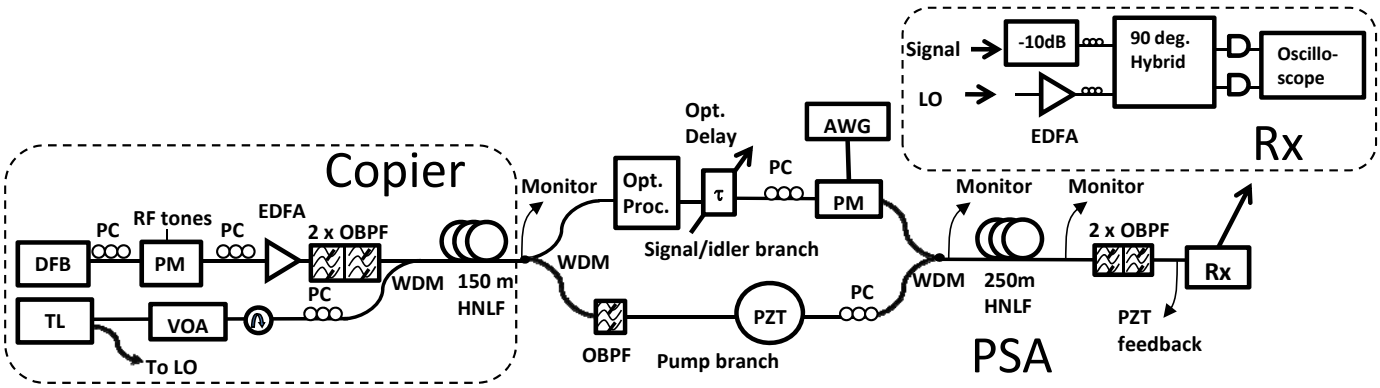

Fig. 11. Schematic setup of the PSA experiment. DFB: Distributed feedback laser, TL: Tunable laser, PC: Polarization controller, PM: phase modulator, EDFA: Erbium doped fiber amplifier, OBPF: optical band pass filter, VOA: variable optical attenuator, WDM: wavelength division multiplexer, HNLF: highly nonlinear fiber, AWG: arbitrary waveform generator, PZT: Piezoelectric transducer. The optical processor (Finisar WaveShaper 1000E) acts as bandpass filters centered around the signal and idler. The signal and idler are then phase-modulated simultaneously. The PSA output is also used as feedback signal to drive the PZT.

Going forward, even more advanced phase-locking schematics will be necessary to enable true black-box phase-sensitive operation. We are considering several ways to do this, using e.g. subsystems based on injection locked lasers.

V. Phase-squeezing in non-degenerate-idler PS-FOPA

A very intriguing property of a phase-sensitive amplifier is that in addition to amplify or deamplify the signal, it will squeeze the optical phase of the signal, depending on its phase. Since the parametric amplifier has an ultra-fast response time on the order of femtoseconds, this effect can for instance be used for phase regeneration of high-speed data signals. Several earlier proof-of-concept demonstrations have been shown in the literature [16], [17], and in [25] a black-box single channel phase regenerator was demonstrated based on this effect. However, the phase squeezing has only been presented in terms of sampled constellation diagrams, and quantified through the signal quality improvement, with the signal artificially distorted by modulation with a sinusoidal signal.

In this study, we present the first experimental investigation of any PSA that includes both phase and amplitude response, as a function of input phase [26]. We also investigate the pump power dependence of the phase-squeezing properties and quantify the squeezing of broadband phase noise. The results were obtained by imposing a linear phase modulation onto the signal and idler wave simultaneously, and detecting the input and output signal using a self-homodyne coherent receiver. It is shown that the phase squeezing is proportional to the PSA gain, in accordance with theory.

The copier+PSA experimental setup was described in section IV. Additionally, the self-homodyne coherent receiver used to detect and characterize the signal was based on a 90° optical hybrid in which the signal and LO (tapped off from the signal laser prior to the copier+PSA setup) was mixed. Finally, the two hybrid outputs, corresponding to the two quadratures of the signal, were detected with two p-i-n photo-receivers and visualized on a 3 GHz bandwidth real-time sampling oscilloscope.

The phase squeezing was measured by phase modulating the signal and idler simultaneously with a sawtooth wave. Fig. 12 shows the optical power (dashed line, logarithmic scale) and phase (solid line) of the signal measured over 45 ns at the output with the idler blocked in the optical processor, giving phase-preserving PI operation (top) and passed through, giving PS operation (bottom). At the input, the power is constant, while the phase linearly varies over all phase states. At the PSA output, the field amplitude is modulated sinusoidally, while the phase is squeezed into two phase states, in accordance with theory. The remaining phase noise around the two output states is attributed to an uncertainty in the relative phase at the PSA input due to the pump phase dithering to suppress SBS. The measurement time was not limited by PSA stability, but by the stability of the self-homodyne coherent receiver.

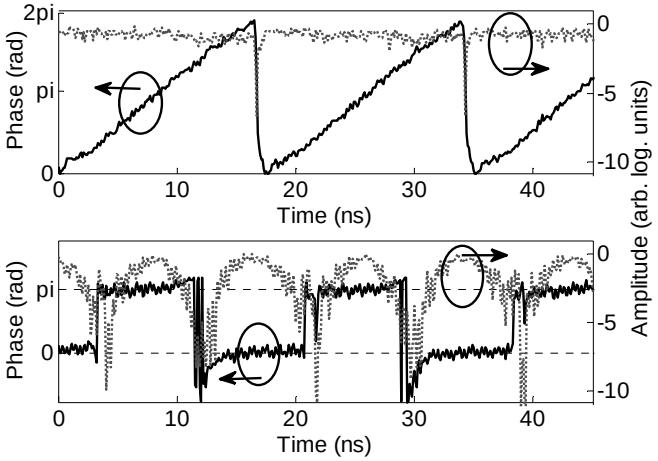

Fig. 12. Signal amplitude (dashed line, logarithmic scale) and phase measured in real time in PI mode (top) and PS mode (bottom).

In Fig. 13, the calculated and measured output phase is shown for different PSA on-off gains, set by changing the pump power. The theoretical and experimental data agree well. It is apparent that the amount of phase squeezing is related to the pump power, and thus the PSA gain. Around the squeezing axis (the two phase states giving maximum gain in the PSA, and the center of the flattest parts in the phase curves); the output phase is compressed by approximately the same factor as the maximum signal gain in the PSA. It should be noted that the relevant measure here is the PSA on-off gain, a lower net gain (for instance due to a large loss in the nonlinear medium) would not impact the phase squeezing.

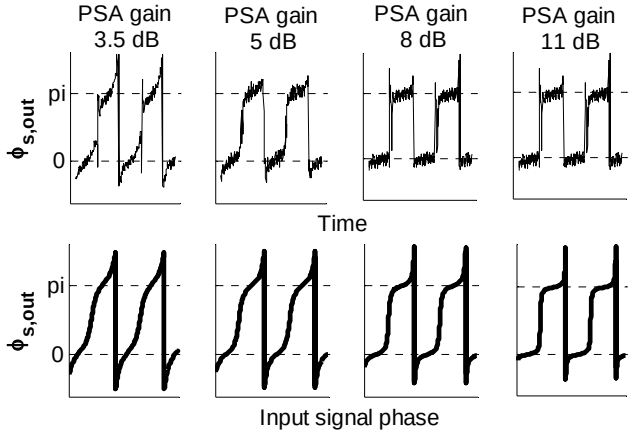

Fig. 13. Measured (top) and calculated (bottom) signal phase for PSA on-off gains of 3.5, 5, 8 and 11 dB, respectively. The calculated phases are plotted versus input phase, the measured phases versus time (the input phase was linearly varied).

Finally, we investigated the reduction of phase noise in a signal distorted by additive white Gaussian noise (AWGN). An electrical square-wave signal with added AWGN (SNR=3dB) was used to drive the PM. The AWG used to generate the signal limited the bandwidth of the signal to around 5 GHz. The optical signal phase measured before and after the PSA is shown in Fig. 4. The PSA gain was about 8 dB. The input signal has less noise at the lower phase level due to clipping of the electrical signal, and spikes in the output phase curve are due to samples that were close to or on the wrong side of the transition phases ($\pm\pi/2$). A histogram of the signal phase is shown in Fig. 5. The standard deviation in the upper phase level is reduced by almost a factor of four which is consistent with the results from Fig. 3. It is believed that the phase squeezing is to some extent obscured by the excess phase uncertainty, resulting from the pump dithering.

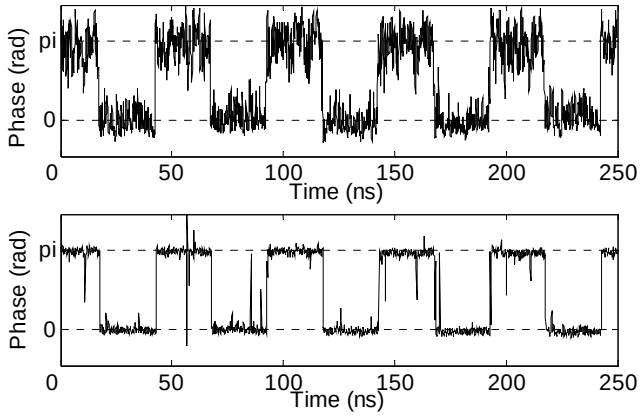

Fig. 14. Signal phase measured in real time before (top) and after (bottom) PSA.

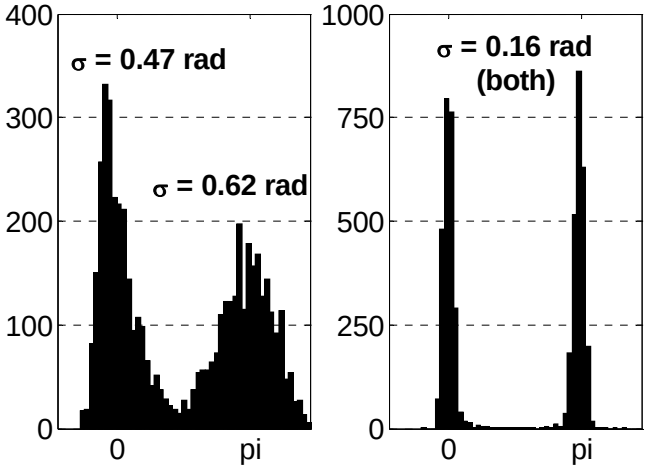

Fig. 15. Histograms of signal phase before (left) and after (right) PSA.

We have invested a substantial amount of time implementing the PS-FOPA setup detailed in Fig. 11. It is based on simultaneous modulation of a cw signal-idler pair. Using a self-homodyne coherent receiver, the signal could be characterized in terms of both phase and amplitude before and after the PSA. We performed the first full experimental investigation of the PSA phase squeezing properties by linearly varying the input phase and measuring the output phase with a coherent receiver. The phase squeezing was shown to be linearly related to the PSA on-off-gain, in accordance with theory. Moreover, we demonstrated the squeezing of broadband phase noise in a PSA for the first time, and showed a reduction of the phase standard deviation by a factor of four. Planned future extensions of this work include the investigation of phase regeneration in a saturated PS-FOPA, which would in principle reduce the conversion of phase noise to amplitude noise due to the phase-sensitive gain.

VI. NF MEASUREMENT OF A CASCADED PS-FOPA WITH SHOT-NOISE LIMITED INPUTS

One problem when measuring the PSA NF in a cascaded PIA + PSA scheme is that the excess noise generated from the PIA stage must be subtracted to meet the requirement of shot-noise-limited inputs. As a result complicated RIN subtraction method is needed in the measurement [27], which makes the experiment less straightforward. As mentioned in our previous report to EOARD, the mid-stage loss will also affect the NF results. In theory shot-noise-limited input can be achieved by using a large attenuation before the PSA, however, it will also heavily decrease the pump power in a straight-line configuration.

We have solved this problem by separating both pump and signal/idler waves after the copier, and then significantly attenuating and equalizing the signal and idler powers before the PSA input. In addition, the gain of the copier stage is very small to avoid excess noise generation. Based on this setup, we have successfully measured the lowest NF reported ever in an optical amplifier with high gain (larger than 10 dB). It should be mentioned that compared with a nonlinear crystal based PSA, the fiber-based solution has less insertion loss, which makes it more practical for real applications.

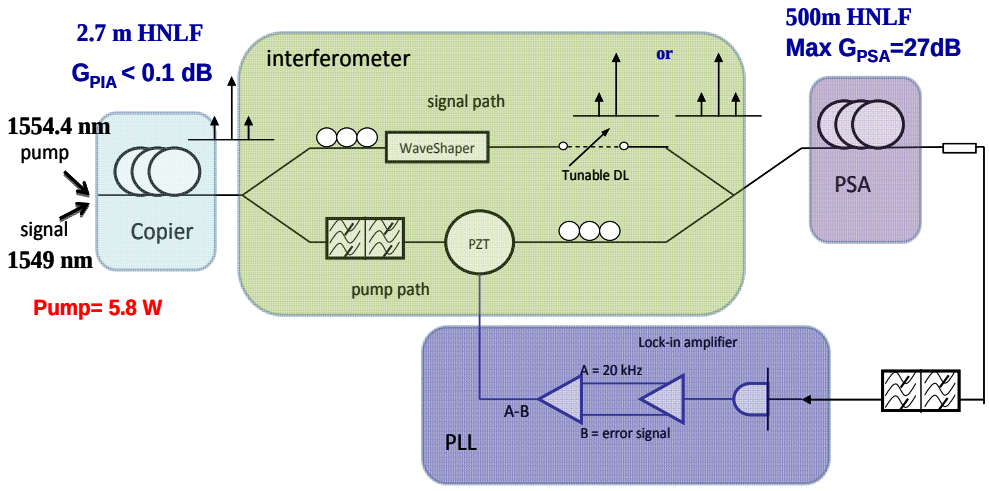

Fig. 16 Experimental setup of the PSA NF measurement with shot-noise-limited inputs.

The experimental setup is shown in Fig. 16, where we used a very short HNLF (2.6 m) as the copier stage, and then separate the pump and signal-idler waves by using a WDM coupler. Through an optical processor we can individually change the amplitude and phase of the signal and idler waves. Finally, signal, idler and pump are combined again by using another WDM coupler, and then input to the PSA stage. A PZT-based phase-locking loop is used to compensate the phase-errors due to the acoustic noise as well as ambient temperature variations. Thanks to the optical processor, we can easily turn on or off the idler wave, which means we can directly compare the performance of the PIA and PSA modes. A 5.9 dB PSA gain improvement has been observed over the PIA mode, and a -1.9 dB ± 0.4 dB signal/idler separate NF (which corresponds to a 1.1 dB 'real' NF) has been measured at a larger than 26 dB PSA gain under the equalized signal/idler input power (signal input is -42 dBm, and the total input is -39 dBm), as shown in Fig. 17. The reason why the NF starts to increase at very low input power is probably due to the residual acoustic noise, which is not completely compensated by the PLL and transferred to intensity noise [28]. Another interesting result is that, by comparing the signal NF in PIA and PSA mode, a larger than 5.3 dB NF difference can be observed. Actually, this is a convincing proof that PSA can have negative separate NF.

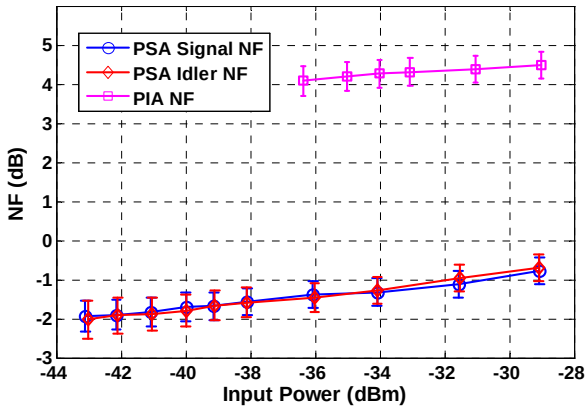

Fig. 17 Measured signal and idler separate NFs in PSA mode as well as signal NF in PIA mode vs. input powers.

We also measured both gain and NF spectra of the low-noise PSA at the maximal gain, which is the first measurement ever to show the broadband capability of a non-degenerate PSA. In Fig. 18, we can clearly find that well below conventional quantum limit noise performance is obtained over 8 nm bandwidth, with larger than 26 dB gain (34 dB gain in the exponential regime). It should be mentioned that the amplification bandwidth is only limited by the waveshaper's bandwidth, and larger amplification bandwidth can be expected if we change to a better optical processor. In theory, a PS-FOPA can have the same bandwidth as a PI-FOPA, while the maximal gain will be about 6 dB higher (in high gain regime) and the minimal separate NF (considering signal or idler wave alone) will be 6 dB lower, as shown in Fig. 19, which directly compares the maximal gain and minimal signal NF in PSA mode and PIA mode at different launched pump power.

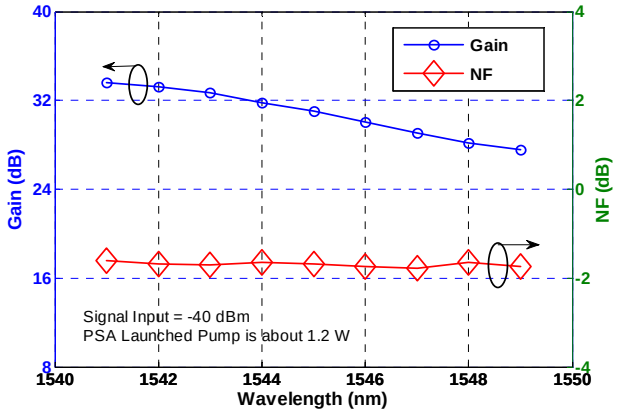

Fig. 18 Measured signal gain and NF spectra of the low-noise non-degenerate PSA.

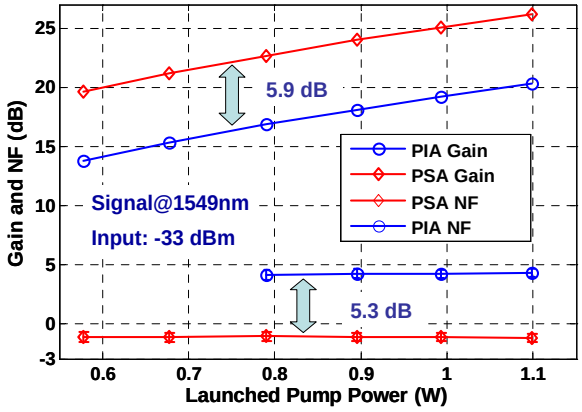

Fig. 19 Comparison of maximal gain and minimal NF in PIA and PSA amplification modes, respectively, through directly suppressing the idler wave.

All the above results are measured under the equalized signal and idler input condition, which is also the default assumption in most previously conducted research. What will happen if the input powers are un-equalized? It should be pointed out that the un-balanced inputs can only be realized in non-degenerate PSAs (two-mode squeezing).

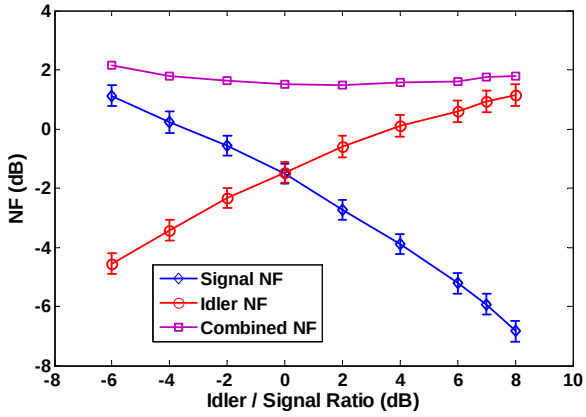

Fig. 20 Measured NF of the low-noise non-degenerate PSA with un-equalized signal-idler inputs. The idler input is fixed at -36 dBm in the experiment.

Considering the signal-idler correlation in the parametric process, both the gain and noise performance of signal and idler are highly correlated. In Fig. 20, the signal and idler separate NF curves have been measured at different idler-to-signal ratio, and the results show that the weaker input will have a better noise performance as well as PSA gain, while the noise performance of the stronger input will be degraded. Thus the optimal NF can be even lower than -3 dB when the inputs are un-equalized, however the combined NF is still above 0 dB, and will reach the minimum at the equalized point. The results clearly show that the combined NF which considers both signal and idler NFs is a reasonable definition of noise performance in a non-degenerate PSA.

VII. TRANSMISSION SYSTEMS UTILIZING PSAS

It is well recognized that PSAs could improve (compared with the use of EDFAs) the noise performance of fiber optical transmission links, however, most previous investigations focused on degenerate PSAs which are inherently single-channel devices and a 3 dB NF improvement can be expected. Considering the very complicated phase-locking scheme required, non-transparent amplification to multi-level phase-coded signals as well as the single channel nature, this 3 dB improvement is not so attractive. A frequency non-degenerate PSA can provide the WDM compatibility, but how to apply such an amplifier in the real link still remains a big challenge, since more complicated phase-control technologies are necessary to build a single-stage non-degenerate PSA. Even though a cascaded copier + PSA scheme needs much less hardware to perform phase-locking as mentioned before, it has to date, neither been considered particularly attractive since the general understanding has been that the cascaded scheme will give a worse noise performance than pure-PSA based links. Apparently, to compete with conventional EDFAs, PSAs should show substantial performance improvement at as low cost and complexity as possible.

Based on our semi-classical model, we have, however, found that if we apply this copier + PSA scheme to the fiber transmission links (as shown in Fig. 21), we will obtain a *6 dB SNR improvement compared to the conventional PIA* amplified links, or 3 dB improvement over the pure-PSA links, when the span number is large enough [29], as shown in Fig. 22. Here, a PI-FOPA is used as the copier in the first span (amplifier + fiber), to amplify the signal as well as to generate the conjugated idler. After the first span, the phase- and wavelength-locked signal, idler and pump waves are input to the following parametric amplifiers, where non-degenerate PS amplification can be achieved. However, to achieve optimal PSA performance (highest gain and lowest NF), several practical issues need to be addressed: (i) The pump power and phase (propagated along the fiber as a pilot tone) must be regenerated with very low phase and intensity noise. This might be realized by using injection locking with a high performance slave laser [30, 31]. (ii) The relative phase between the pump, signal and idler should be precisely manipulated to obtain the maximal PS gain, thus requiring perfect dispersion and dispersion slope compensation plus accurate phase-shifting. The simplest method is to use a piece of SMF with proper length [32]. However, for WDM applications, per-channel phase control is needed. Liquid-crystal [33] or MEMS [34] based frequency-resolved phase shifters might be good choices in such a situation. (iii) Polarization tracking and adaptive control are required at the input of each FOPA since parametric amplification is highly polarization-dependent [35]. (iv) Phase locking might be required for recombining the regenerated pump and the signal/idler wave before the PSAs, as shown in Fig. 2, to cancel the slowly-varying phase-errors induced by environmental fluctuations or temperature changes. Of course the system performance will be much better if the above functions can be integrated together. A qualitative explanation for this counter-intuitive SNR performance improvement when using the copier relies on two important points. Firstly, in a long-haul transmission system with many spans, most of the noise is induced by the fiber loss, and the noise contribution from the first PI-FOPA will become less important. Secondly, for such a cascaded copier + PSA link, only the signal wave should be considered to obtain the NF (as there is no idler at the link input), thus the NFs of the following PSAs can be regarded to be -3 dB when the fiber loss is substantial (assuming coherent inputs into each PSA). This is the optical transmission link with the best noise performance ever reported. Obviously, this 6 dB SNR improvement means quite a lot for high-capacity transmission systems, e.g. a transmission distance increase by a factor of 4, or 4 times lower input signal power at the same transmission length (thereby also reducing the impact of fiber nonlinearities).

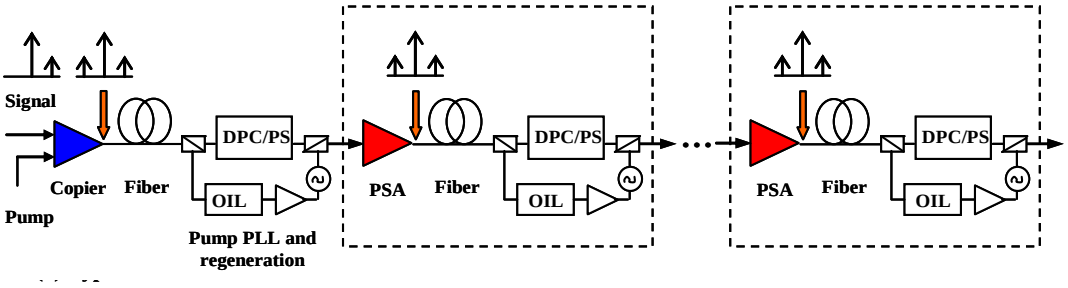

Fig. 21 Schematic of copier + PSA amplified multi-span transmission link. DPC/PC: Dispersion and polarization compensation / Phase shifter; OIL: Optical injection-locked laser; PLL: Phase locking loop.

In addition, other than the best SNR performance as well as the relative simple structure, the proposed copier + PSA scheme is also WDM compatible, modulation format independent, and polarization multiplexing possible, which makes it very promising for future ultra-high capacity coherent transmission systems that require high SNR. Moreover, this scheme can support distributed amplification, which could give even better performance for ultra-long haul transmission systems.

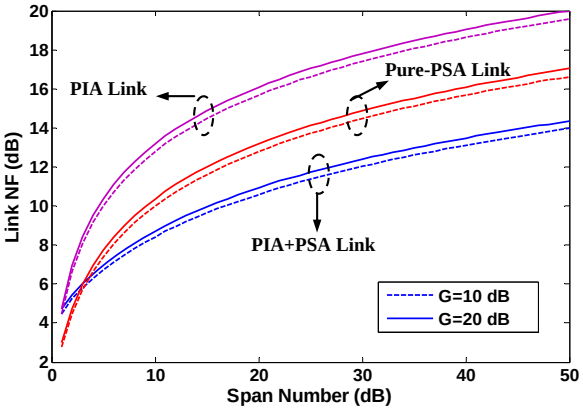

Fig. 22 Calculated link NF vs. the span number for the cascaded PIA +Fiber + PSA + Fiber + PSA + …, pure-PIA and pure-PSA transmission systems at different link gains.

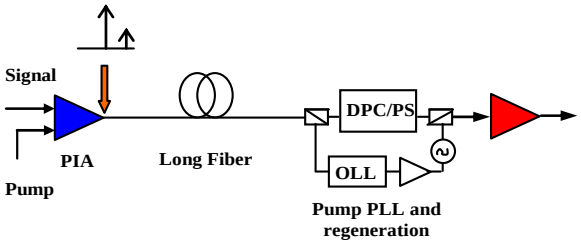

Fig. 23 Schematic of copier + PSA amplified ultra-long haul single-hop transmission.

Other than the multi-span PSA transmission system, the 6 dB NF benefit can also be obtained from another relatively simple scheme – ultra-long haul single-hop PSA transmission, as shown in Fig. 23. In fact, this scheme can be easily realized by replacing a high gain copier stage in Fig. 10, and using the wave-shaper attenuation representing the fiber loss. With a 15 dB copier gain, 21 dB PSA gain and 36 dB inter-stage loss, we have experimentally proved the theoretical concept and for the first time successfully demonstrate the 6 dB NF improvement. In Fig. 24, a larger than 5.5 dB NF advantage can be observed over 8 nm bandwidth, compared to the pure-PIA amplification (by suppressing the idler) as well as the EDFA amplification with the same gain.

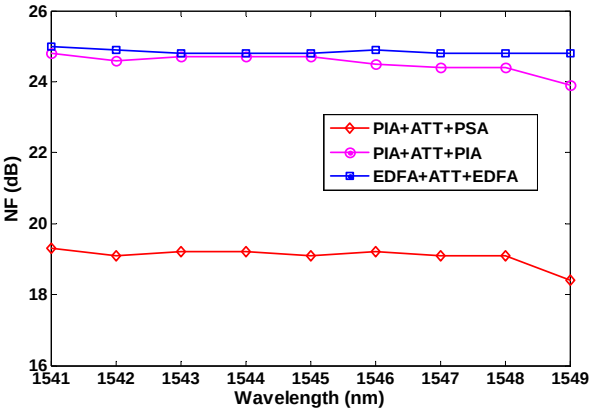

Fig. 24 Measured total NF spectra of the copier+attenuation+PSA, copier+attenuation+PIA, and EDFA+attenuation+EDFA schemes. The net gain is identical for all three schemes.

Furthermore, we also demonstrated the WDM compatibility of the proposed copier + PSA scheme in Fig. 25. By monitoring the middle channel to phase-lock the interferometer, we can easily achieve stable PSA amplification of the other two channels. The channel spacing is 0.8 nm, and the optimal amplification is derived through modifying the channel phase separately (via the optical processor). It should be mentioned here that the input signals are from free-running lasers, which is the first demonstration of WDM amplification of non-degenerate PSAs at arbitrary channel spacing.

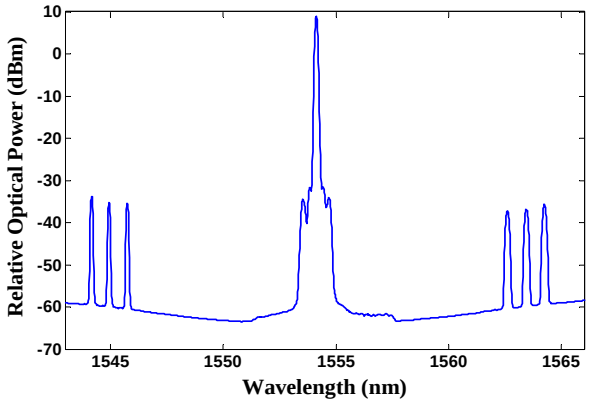

Fig. 25 Output PSA spectrum of WDM signals.

VIII. CONCLUSIONS

We have demonstrated several new developments in the field of FOPAs. By using a high pump and signal power, a high power CW idler outside of the conventional C/L-band EDFA gain bandwidth was generated. These waves were subsequently used to implement a dual-pumped FOPA with ultra-high pump separation, and its gain was shown to be limited by fundamental fiber properties. We have also detailed recent advances in the understanding of noise figure performance of FOPAs, including full spectral NF measurements of a single-pumped FOPA, showing the Raman induced asymmetric characteristic. Finally, we have also presented our recent and ongoing work on phase-sensitive FOPAs based on PI- and PS-FOPAs in cascade. We have measured the gain and the NF of the PSA, and have demonstrated phase squeezing in a non-degenerate-idler PS-FOPA. A record NF = 1.1 dB was measured in a high-gain (26 dB) PS-FOPA. We are currently investigating various applications of PS-FOPAs, including in transmission systems. Based on the content in this report, we feel increasingly confident that the techniques reported here will find interesting applications in the future.

REFERENCES

[1] J. Hansryd and P. A. Andrekson, "Broadband CW pumped fiber optical parametric amplifier with 49 dB gain and wavelength conversion efficiency," *IEEE Photon. Technol. Lett.*, vol. 13, pp. 194–196, Mar. 2001.

[2] M. E. Marhic, K. K. Y. Wong, and L. G. Kazovsky, "Wide-band tuning of the gain spectra of one-pump fiber optical parametric amplifier," *J. Sel. Top. Quantum Electron*., vol. 10, no. 5, pp. 1133–1141, Sep.-Oct. 2004.

[3] T. Torounidis and P. A. Andrekson, "Fiber-based parametric amplifier with 70 dB gain", *IEEE Photon. Technol. Lett.*, vol. 18, no. 10, pp. 1194–1196, May 2006.

[4] W. Imajuku, A. Takada, and Y. Yamabayashi, "Inline coherent optical amplifier with noise figure lower than 3dB quantum limit," *Electron. Lett.*, vol. 36, no. 1, Jan. 2000.

[5] T. Torounidis, H. Sunnerud, P. O. Hedekvist, and P. A. Andrekson, "Amplification of WDM signals in fiber-based optical parametric amplifiers," *IEEE Photon. Technol. Lett.*, vol. 15, no. 8, pp. 1061–1063, Aug. 2003.

[6] J. Hansryd et al., "Fiber-based optical parametric amplifiers and their applications," *J. Sel. Top. Quantum Electron*., vol. 8, pp. 506–520, May-June 2002.

[7] J M C Boggio, C. Lundström, J Yang, H Sunnerud and P. A. Andrekson, "Double-pumped FOPA with 40 dB flat gain over 81 nm bandwidth," in *Proceedings European Conference on Optical Communication (ECOC)*, Paper Tu.3.B.5, Brussels, 2008.

[8] Z. Tong, C. Lundström, M. Karlsson and P. A. Andrekson, "Noise figure non-reciprocity in fiber parametric amplifiers with zero-dispersion-wavelength variations," accepted by *ECOC'2010*, Torino, Italy, 2010.

[9] Z. Tong, A. Bogris, M. Karlsson and P. A. Andrekson., "Full characterization of the signal and idler noise figure spectra in single pumpedfiber optical parametric amplifiers," *Opt. Exp.*, vol. 18, pp. 2884-2893, Feb. 2010.

[10] M. Karlsson, "Four-wave mixing in fibers with randomly varying zero-dispersion wavelength," *J. Opt. Soc. Am. B*, vol. 15, pp. 2269-2275, Aug. 1998.

[11] P. Velanas, A. Bogris and D. Syvridis, "Impact of dispersion fluctuations on the noise properties of fiber optical parametric amplifiers," *J. Lightwave Technol.* vol. 24, pp. 2171-2178, May 2006.

[12] M. Marhic, G. Kalogerakis and L. Kazovsky, "Gain reciprocity in fibre optical parametric amplifiers," *Electron. Lett.*, vol. 42, pp.519-520, 2006.A. Bogris and D. Syvridis, "RZ-DPSK Signal Regeneration Based on Dual-Pump Phase-Sensitive Amplification in Fibers," IEEE Photon. Technol. Lett. **18**, 2144-2146 (2006).

[13] E. Myslivets, et al., "Spatial equalization of zero-dispersion wavelength profiles in nonlinear fibers," *IEEE Photon. Technol. Lett.*, vol. 21, pp. 1807-1809, Dec. 2009.

[14] H. A. Haus and J. A. Mullen, "Quantum Noise in Linear Amplifiers," Physical Review **128**, 2407 (1962).

[15] A. Bogris and D. Syvridis, "RZ-DPSK Signal Regeneration Based on Dual-Pump Phase-Sensitive Amplification in Fibers," IEEE Photon. Technol. Lett. **18**, 2144-2146 (2006).

[16] K. Croussore, I. Kim, Y. Han, C. Kim, G. Li, and S. Radic, "Demonstration of phase-regeneration of DPSK signals based on phase-sensitive amplification," Opt. Express, **13**, 3945-3950 (2005).

[17] K. Croussore and G. F. Li, "Phase and amplitude regeneration of differential phase-shift keyed signals using phase-sensitive amplification," IEEE J. of Sel. Top. Quantum Electron. **14**, 648-658 (2008).

[18] L. Ruo-Ding, P. Kumar, and W. L. Kath, "Dispersion Compensation with Phase-sensitive Optical Amplifiers, "IEEE J Lightwave Technol.**12**, 541-549 (1994).

[19] M. E. Marhic, Y. Park, F. S. Yang, and L. G. Kazovsky, "Widely tunable spectrum translation and wavelength exchange by four-wave mixing in optical fibers," Opt. Lett. **21**, 1906-1908 (1996).

[20] K. Croussore and G. Li, "Amplitude regeneration of RZ-DPSK signals based on four-wave mixing in fibre," Electron. Lett. **43**, 177-178 (2007).

[21] M. Sköld, J. Yang, H. Sunnerud, M. Karlsson, S. Oda, and P. A. Andrekson, "Constellation diagram analysis of DPSK signal regeneration in a saturated parametric amplifier," Opt. Express, **16**, 5974-5982 (2008).

[22] M. E. Marhic, C. H. Hsia, and J. M. Jeong, "Optical amplification in a nonlinear fibre interferometer," Electron. Lett **27,** 210-211 (1991).
[23] M. Vasilyev, "Distributed phase-sensitive amplification," Opt. Express **13**, 7563-7571 (2005).
[24] C. Lundström, J. Kakande, P. A. Andrekson, Z. Tong, M. Karlsson, P. Petropoulos, F. Parmigiani, and D. J. Richardson, "Experimental Comparison of Gain and Saturation Characteristics of a Parametric Amplifier in Phase-sensitive and Phase-insensitive Mode," in *Proceedings of European Conference on Optical Communications (ECOC)*, Paper Mo.1.1.1, Vienna, 2009
[25] F. Parmigiani, R. Slavík, J. Kakande, C. Lundström, M. Sjödin, P.A. Andrekson, R. Weerasuriya, S. Sygletos, A. D. Ellis, L. Grüner-Nielsen, D. Jakobsen, S. Herstrøm, R. Phelan, J. O'Gorman[5], A. Bogris, D. Syvridis, S. Dasgupta, P. Petropoulos, and D. J. Richardson, "All-optical phase regeneration of 40 Gbit/s DPSK signals in a black-box phase-sensitive parametric amplifier," in *Optical Fiber Communications Conference*, post-deadline paper PDPC3 (2010)
[26] C. Lundström, B.J. Puttnam, Z. Tong, M. Karlsson and P.A. Andrekson, "Experimental characterization of the phase-squeezing properties of a phase-sensitive parametric amplifier in non-degenerate idler configuration," in *Proceedings of European Conference on Optical Communications (ECOC)*, Torino, 2010
[27] Z. Tong, A. Bogris, C. Lundström, C. J. McKinstrie, M. Vasilyev, M. Karlsson, and P. Andrekson, "Modeling and measurement of the noise figure of a non-degenerate cascaded phase-sensitive fiber parametric amplifiers," *Opt. Express*, **18**, pp. 14820-14835 (2010).
[28] A. Bogris, D. Syvridis and C. Efstathiou, "Noise properties of degenerate dual-pump phase sensitive amplifiers," J. Lightwave Technol., in press.
[29] Z. Tong, C. J. McKinstrie, C. Lundström, M. Karlsson, and P. Andrekson, "Noise performance of optical fiber transmission links that use non-degenerate cascaded phase-sensitive amplifiers," *Opt. Express*, **18**, pp. 15426-15439 (2010).
[30] A. Takada and W. Imajuku, "In-line optical phase-sensitive amplifier employing pump laser injection locked to input signal light," Electron. Lett. **34**, 274-276 (1998).
[31] R. Weerasuriya, S. Sygletos, S. K. Ibrahim, R. Phelan, J. O'Carroll, B. Kelly, J. O'Gorman and A. D. Ellis, "Generation of frequency symmetric signals from a BPSK input for phase sensitive amplification," in *Optical Fiber Communications Conference*, paper OWT6 (2010).
[32] R. Tang, L. Jacob, P. S. Devgan, V. S. Grigoryan, P. Kumar and M. Vasilyev, "Gain characteristics of a frequency nondegenerate phase-sensitive fiber-optic parametric amplifier with phase self-stabilized input," Opt. Express **13**, 10483-10493 (2005).
[33] G. Baxter, S. Frisken, D. Abakoumov, H. Zhou, I. Clarke, A. Bartos and S. Poole, "Highly programmable wavelength selective switch based on liquid crystal on silicon switching elements," in *Optical Fiber Communication Conference*, paper OTuF2 (2009).
[34] G. Zhou and F. S. Chau, "Nondispersive optical phase shifter array using microelectro-mechanical systems based gratings," Opt. Express **15**, 10958-10963 (2007).
[35] C. J. McKinstrie, H. Kogelnik, R. Jopson, S. Radic, and A. Kanaev, "Four-wave mixing in fibers with random birefringence," Opt. Express **12**, 2033-2055 (2004).